CERN EUROPEAN ORGANISATION FOR NUCLEAR RESEARCH

DESIGN AND PERFORMANCE OF A LIQUID SCINTILLATOR/IRON SANDWICH CALORIMETER USED AT THE ISR

L. BAUM, H. HILSCHER, F. LOBKOWICZ*), C. RUBBIA, A. STAUDE.
CERN, Geneva, Switzerland, Harvard University, Cambridge, Mass., and Sektion Physik der Universität, München, Germany.

ABSTRACT

A liquid scintillator/iron sandwich calorimeter consisting of 12 identical modules and with 3 mm sampling has been built. Its total length corresponds to 6 absorption lengths and its lateral size is 125 x 80 cm^2. The module is viewed by two phototubes, one on each side. The light extraction is based on a new technique developed by one of the authors. The calorimeter was tested in a negative beam at several momenta between 4.5 and 17.2 GeV/c. The energy resolution for pions in this momentum range varies from σ = 20% at 4.5 GeV/c to σ = 11% at 17.2 GeV/c. The energy response is linear and the pulse height distribution is Gaussian. The modular structure provides the possibility of particle identification and the difference in pulse height of the left and right side of each module permits the localization of the center of the shower along the direction of incident particles.

Geneva - 5 Mai 1975

---

*) On leave from the University of Rochester, Rochester, NY.

1. INTRODUCTION

Calorimeter is the popular name for a total absorption spectrometer which measures the energy of an incoming particle by detection of some fractional ionisation loss of that particle and all the produced secondaries. Most calorimeters used at high energies are stacks of plates of dense material to provide for the stopping power, and scintillators for the ionisation measurement. Compared to magnetic spectrometers, calorimeters have the advantage of low cost, being usable for neutral as well as for charged particles, measuring the energy of single particles or particle jets, and providing an instantaneous fast signal with an amplitude proportional to the incident particles' energy. The energy resolution for calorimeters is inferior to that of magnetic spectrometers. However, it improves with increasing energy, contrarily to the performance of magnetic spectrometers.

We have built a liquid scintillator/iron calorimeter of 1 m^2 cross section to be used at the CERN-ISR. Since we were mainly interested in relatively low energy particles (10 to 30 GeV) we paid particular attention to good resolution at low energy. Therefore we have chosen a fine ionisation sampling of 3 mm (3 mm steel/3 mm scintillator-sandwiching) [1,2].

The calorimeter consists of 12 identical modules which permits the study of the shower development along the incident particle's trajectory. The different response to hadrons, electrons and muons can therefore be used to distinguish different particles. Furthermore, each module is viewed by two phototubes, The difference of pulse heights of the two tubes determines the impact point of the measured particle.

The calorimeter has been tested in a negative beam at the CERN-PS in the momentum range of 4.5 to 17.2 GeV/c. We report here on the design of the calorimeter and on the results of this test.

2. DESCRIPTION OF THE CALORIMETER

2.1 Mechanical Design

The calorimeter consists of 12 identical modules. Each module (fig. 1) is a set of 26 iron plates, 3 mm thick, spaced 3 mm apart. The gaps between the plates are filled with liquid scintillator of the type NE 235, a scintillator on mineral oil basis with a light output of about 2/3 of a typical plastic scintillator. The total thickness of the module is 68 g/cm^2 which corresponds to about half an absorption length and 4.5 radiation lengths. About 14% of the ionisation energy is dissipated in the liquid scintillator. The lateral dimensions are 125 x 80 cm^2. The two short sides are closed by conically shaped solid plexiglass light guides which collect the light emerging from the gaps onto the 5 inch photocathode of a 58 DVP photomultiplier. The whole package of plates and light guides are bolted and glued together forming a liquid tight rigid block of about 950 Kp weight.

2.2 Optical properties

The problem of extracting the light out of the narrow gaps over distances of more than one meter was solved by following a technique developped at the Harvard University [3]. It is based on internal reflection on an aluminized teflon foil of 25 μ thickness with which the iron plates have been coated on both sides (fig. 2). Teflon has a refractive index of n = 1.35 compared to n = 1,47 of the scintillator liquid. This corresponds to an angle of internal reflection of about 24^o with respect to the teflon surface. The liquid contains a wave length shifter component which converts the UV light into the frequency region where the photocathode is sensitive. The aluminum layer between the teflon foil and the iron plate is to increase the mean path length of the light to be shifted. The space dependence of the light collection was measured with traversing muons (see chap. 3) by moving the calorimeter horizontally and vertically in the beam. The results are shown in figs 3a-c. The collection efficiency varies rapidly with the horizontal position for one phototube but slowly for the sum of the left and right signals within the fiducial volume of the shower containment of

about 80 cm horizontally. Although the measurements were not very precise because of the spread of the muon beam and a badly defined beam line the results agree rather well with what we expected from calculations.

3. TEST SET UP AND MEASUREMENTS AT THE CERN PS

The calorimeter was tested in a negative pion beam with a maximum momentum of 17.2 GeV/c. Pulse height spectra were measured at 4.5, 8, 11, 14 and 17.2 GeV/c. Fig. 4 shows the schematic experimental layout. The calorimeter was positioned just in front of the beam dump. The beam enters frcm the left. An incoming particle was defined by a coincidence signal of two small scintillation counters T1 and T2 and no signal from the counters A1 and A2 which covered a large fraction of the front side of the calorimeter and which eliminated multiparticle events. The pulse height information of two additional counters PH1 and PH2 were softwarewise used for better single particle definition and to detect escaping particles. The beam was contaminated by a small fraction of muons and some electrons at low momenta. Muons were identified by a coincidence signal of a scintillation counter T3 behind the beam dump. At 4.5 GeV a Cerenkov counter signal permitted electron identification.

The gain of the 24 photomultipliers of the calorimeter was equalized by comparing the pulse height distributions for muons which traversed the calorimeter along the axis. The energy resolution for a minimum ionizing particle was measured to be 70% FWHM in one module and 22% FWHM for the sum over all 12 modules (fig. 5). The gain stability was continuously monitored by short muon runs.

The anode signals of the 24 phototubes of the calorimeter as well as some counter signals were digitised by CAMAC ADCs, and written on magnetic tape by a Hewlett Packard on line computer.

4. ENERGY RESOLUTION AND LINEARITY

The pulse height distributions for 17.2, 11 and 4.5 GeV/c pions are shown in a linear scale in fig. 6 and for 17.2 GeV in a logarithmic scale in fig. 7. The resolution is σ = 11.5% at 17.2 GeV/c and σ = 20% at 4.5 GeV/c. Studying the shower development in the modules we observed for a fraction of events a huge spike of energy loss in only one module. This is explained as a large local electro-magnetic component of the shower. As these showers with a strong electro-magnetic contribution dissipate more "visible" (see below and ref. 1) energy the total pulse height for this class of events is higher. This is shown in table 1. One can correct for this effect and thus slightly improve the energy resolution: σ(17.2 GeV/c) = 10.7%. Although σ is not very much changed the pulse height distribution approaches an almost perfect Gaussian distribution (see table 2). Fig. 8 shows the results in comparison with similar detectors. The response of the calorimeter is linear in energy in the measured range. The resolution is considerably better at lower energies than the one by Engler et al., [3] which has 2 cm iron plates.

We determined the fraction of incident energy which is converted to measurable ionisation ("visible energy") to be about 75%. The missing part is essentially lost in nuclear binding and light output saturation ("quenching"). The fluctuations in this fraction is one major effect which determines the energy resolution for hadrons. Electrons are not subject to nuclear interactions and therefore the energy response to electrons is different. At 4.5 GeV/c the π^- beam contained some electrons which were selected to study the energy response. The mean pulse height is about 40% higher than for pions, and the energy resolution is twice as good as for hadrons (fig. 9).

5. EFFECT OF THE SHOWER DEVELOPMENT ON THE PERFORMANCE

5.1 Shower containment

The thickness of iron which is necessary to absorb all the energy and the effect of escaping energy on the resolution has been determined. At 17.2 GeV/c one needs more than 90 cm and at 4.5 GeV/c more than 80 cm thickness of iron to contain the whole shower (fig. 10). The leakage at the back of this calorimeter is of the order of a percent at 17.2 GeV/c. Laterally there is no escape of energy in this calorimeter if the impact point of the incident particle is more than 20 cm away from the edge, the particle trajectory being approximately orthogonal to the plates. The lateral shower containment is shown in fig. 11.

5.2 Particle Identification

The different response of a calorimeter to hadrons, electrons and muons allows the separation of different particles. The modular construction of this calorimeter is well suited to study particle identification.

Hadronic showers develop over several modules with an average fractional energy loss/module of 10% over 5 modules. The maximum mean energy deposition occurs in the third module (fig. 12). There are big fluctuations in the position of the shower beginning and in the longitudinal distribution of the energy dissipation. The range of an electromagnetic shower induced by an electron, however, is much shorter and the shower starts right in the beginning of the calorimeter.

We took advantage of this different behaviour of hadronic and electromagnetic showers in order to clean up a small sample of electron events selected by means of a Cerenkov counter far upstreams in the beam (see fig. 9).

Demanding one minimum ionising particle in every module the identification of muons with this calorimeter is more efficient than any pure absorption technique where one is faced with punch through problems. The number of pions which traverse a certain depth of the calorimeter as minimum ionising particles before they start showering falls off exponentially with traversed

thickness (fig. 13). The absorption length is about 16 cm Fe equivalent. This number slightly depends on the energy cuts which define a single minimum ionising particle. The rejection power for pions against muons with 10 modules of the calorimeter is found to be better than 10^{-3} at 17.2 GeV/c.

In our present experiment at the ISR at CERN the described calorimeter is in fact used as a muon identifier.

6. SHOWER LOCALIZATION IN THE CALORIMETER

An important feature of the modular structure of the calorimeter and light collection on both sides is the possibility to localize the energy flow through the calorimeter. The pulse height of the single phototube depends strongly on the position of the ionisation source whereas the sum of the pulse heights of the left and right phototube varies slowly over a large area (fig. 3). The difference of the left and right pulse height therefore measures the horizontal (X-) coordinate of the shower center. We define for each modul a coordinate

$$X_i = \frac{PH^i_{left} - PH^i_{right}}{PH^i_{left} + PH^i_{right}} \; ; \; i = 1,\ldots 12.$$

where PH^i is the pulse height in module i. This coordinate is only well determined in modules where the energy dissipation is large. Therefore we attribute to the coordinates X_i a weight factor

$$W_i = \frac{PH^i_{left} + PH^i_{right}}{\sum_{i=1}^{12} PH_i}$$

proportional to the fractional energy deposition. The X-distributions at the beginning of the shower for 3 different beam positions are shown in figure 14. The mean value of the distribution varies linearly with the displacement of the shower. The spatial resolution is 11 cm FWHM. The direction of the incoming particle can be determined by fitting a straight line through the coordinates of those modules which contributed to the shower detection. The measured angular resolution was about σ = 100 mrad using only the pulse height informations of the calorimeter.

ACKNOWLEDGEMENT

We would like to thank numerous members of the CERN-Munich-Cracow collaboration for help and support during the measurements and the staff of the CERN-PS for the valuable cooperation. We benefited much from the steady interest and support of Dr. F. Muller during the construction period. The excellent technical assistance of Mr. Herbert and the support of the TC workshop is highly appreciated.

This work was partially supported by the Bundesministerium für Forschung und Technologie.

REFERENCES

(1) Review article about resolution determining factors:
William J. Willis, BNL 17071.

(2) J. Engler, W. Flanger, B. Gibbard, F. Mönning, K. Runge and H. Schopper,
Nucl. Instr. and Meth. 106 (1973) 189.

(3) Private communication and R. Wagner, Technical Memorandum of
Oct. 8, 1973, Harvard University.

(4) Private communication.

TABLE 1

	FRACTION OF TOTAL ENERGY LOSS IN ONE MODULE	FRACTION OF TOTAL NUMBER OF EVENTS	RELATIVE SHIFT OF PULSE HEIGHT
17.2 GeV/c π^-	> 50%	5.6 %	1.07
	40÷50 %	25.4 %	1.04
	30÷40 %	42.0 %	1.00
	20÷30 %	25.4 %	0.97
	< 20%	1.6 %	0.94

TABLE 2

π^-	σ	FRACTION OF TOTAL NUMBER OF EVENTS IN PULSE HEIGHT INTERVAL		
		$\pm\sigma$	$\pm 2\sigma$	$\pm 3\sigma$
17.2 GeV/c uncorrected	11.5 %	65 %	89 %	98 %
17.2 GeV/c corrected	10.7 %	68 %	93 %	99 %
GAUSS		68.3 %	95.4 %	99.7 %

FIGURE CAPTIONS

Fig. 1 Artist's view of a module of the calorimeter.

Fig. 2 Cross section of a gap to explain the principle of light extraction.

Fig. 3 Space dependence of the light collection of a module
a) horizontal scan with one phototube
b) horizontal scan with both phototubes
c) vertical scan with both phototubes.

Fig. 4 Scheme of the experimental layout for the test of the calorimeter in a negative beam at the CERN proton synchroton.

Fig. 5 Pulse height distribution for traversing muons (sum spectrum).

Fig. 6 Pulse height distributions for negative pions at 4.5, 11 and 17.2 GeV/c plotted in a linear scale.

Fig. 7 Pulse height distribution for 17.2 GeV/c π^- plotted in a logarithmic scale.

Fig. 8 Linearity and fractional energy resolution (σ), comparison with other calorimeters:
- iron/plastic scintillator calorimeter (20 mm/7 mm), ref. 2.
- iron/liquid argon calorimeter (1.5 mm/2 mm), ref. 4.

Fig. 9 Comparison of the energy response for π^- and e at 4.5 GeV/c. Plot of pulse height distributions for π^- and e on the same scale.

Fig. 10 Shower containment as a function of total iron thickness. Pulse height and resolution dependence on thickness of iron for 17.2 GeV/c and 4.5 GeV/c negative pions.

Fig. 11 Lateral shower containment. Relative pulse height as a function of the pion impact point from the edge.

Fig. 12 Mean fractional energy deposition (E_i/E_o; i=1...12; $E_o = \sum_{i=1}^{12} E_i$) in each module.

Fig. 13 Determination of the absorption length for 17.2 GeV/c pions in iron. It is plotted the number of pions which traversed a certain thickness of iron without producing secondary particles. The plot also demonstrates the rejection for muons against pions using the calorimeter as a muon identifier.

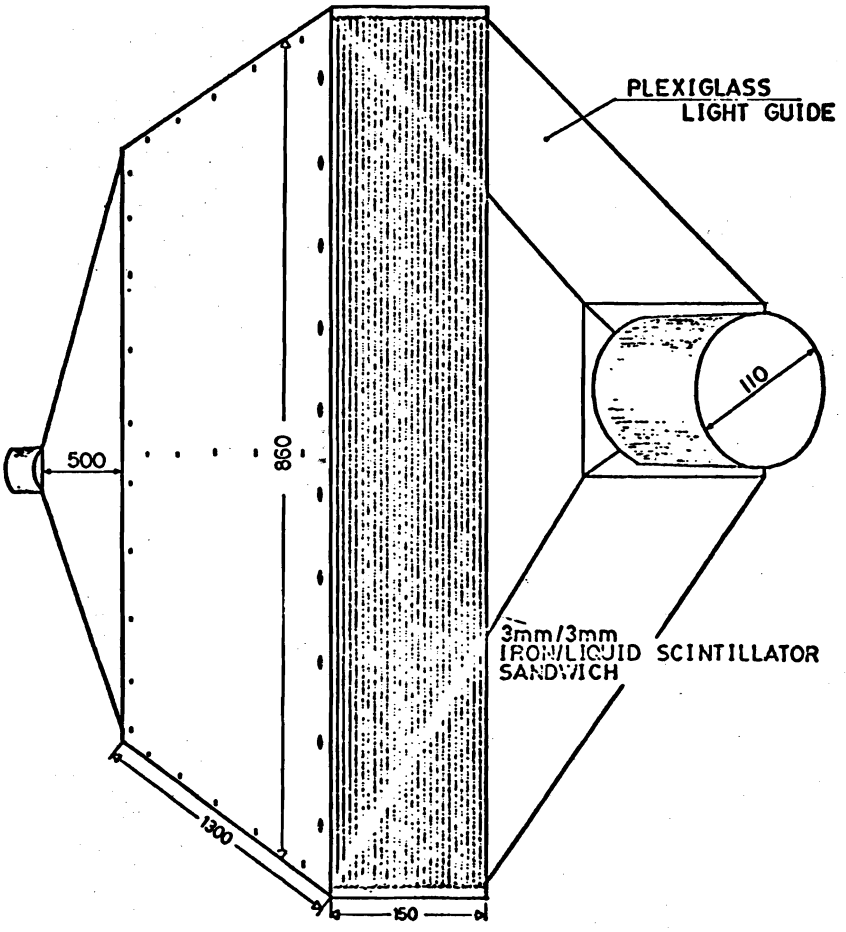
PLEXIGLASS
LIGHT GUIDE
110
500
860
3mm/3mm
IRON/LIQUID SCINTILLATOR
SANDWICH
1300
150

Fig. 1

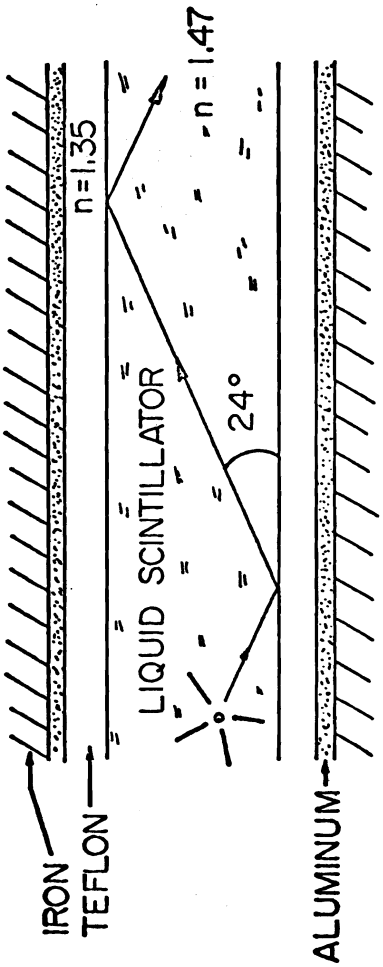

Fig. 2

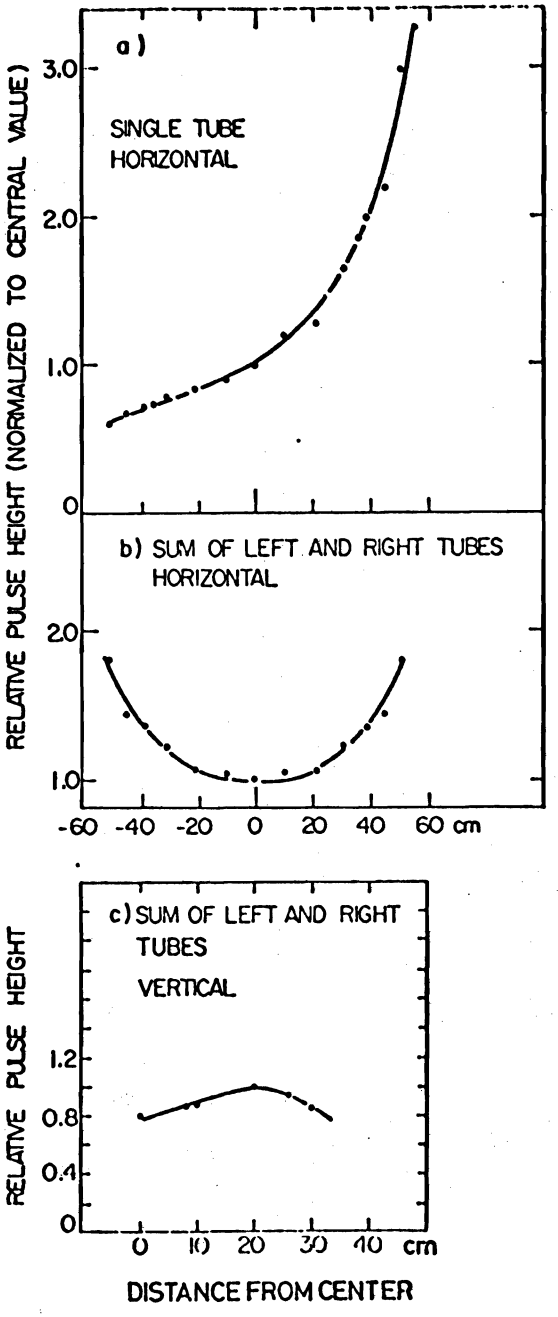
a)
SINGLE TUBE
HORIZONTAL
3.0
2.0
1.0
0
b) SUM OF LEFT AND RIGHT TUBES
HORIZONTAL
2.0
1.0
-60 -40 -20 0 20 40 60 cm
RELATIVE PULSE HEIGHT (NORMALIZED TO CENTRAL VALUE)
c) SUM OF LEFT AND RIGHT
TUBES
VERTICAL
1.2
0.8
0.4
0
0 10 20 30 40 cm
RELATIVE PULSE HEIGHT
DISTANCE FROM CENTER

Fig. 3

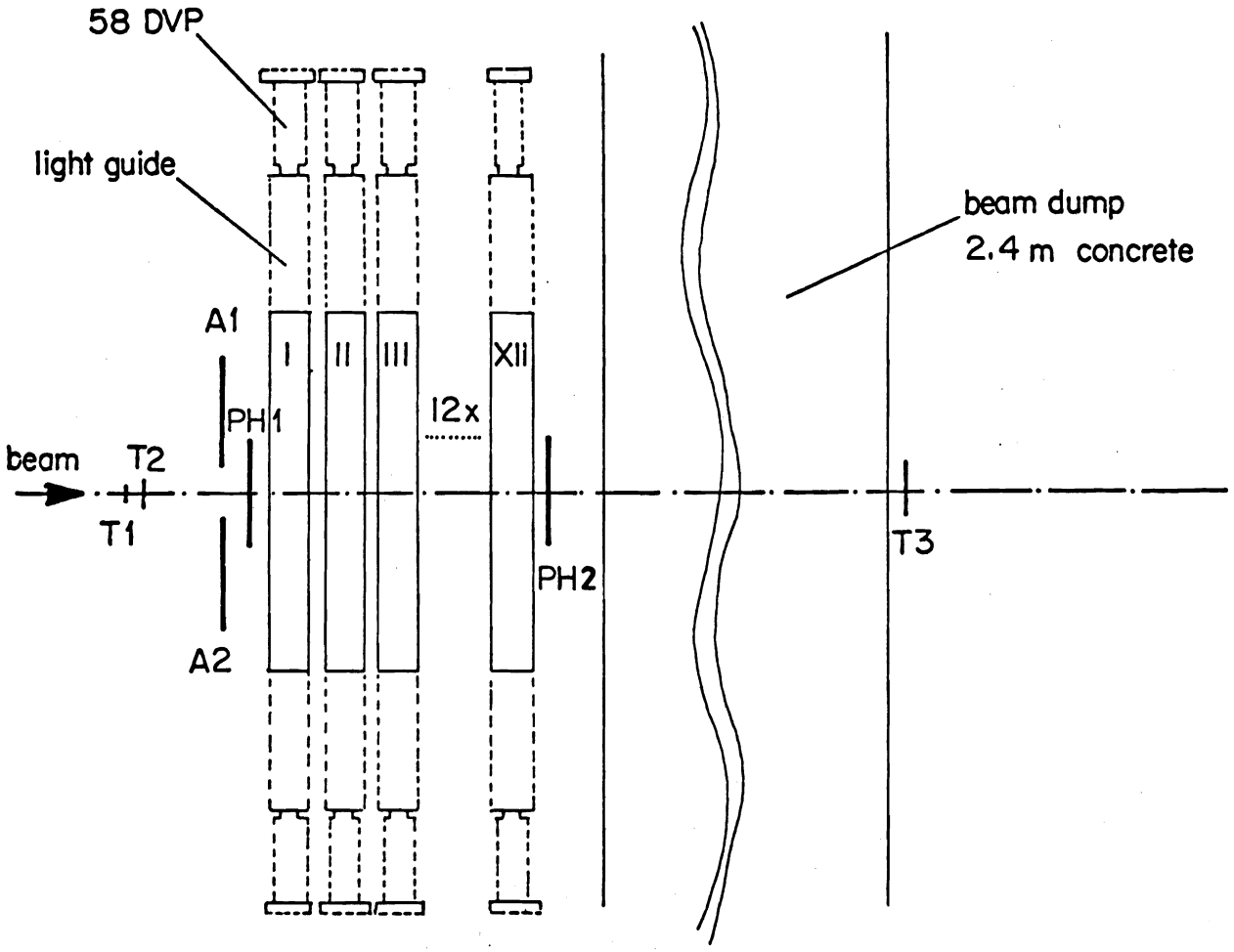
58 DVP
light guide
beam dump
2.4 m concrete
A1
I
II
III
XII
12x
PH1
beam
T2
T1
A2
PH2
T3

Fig. 4

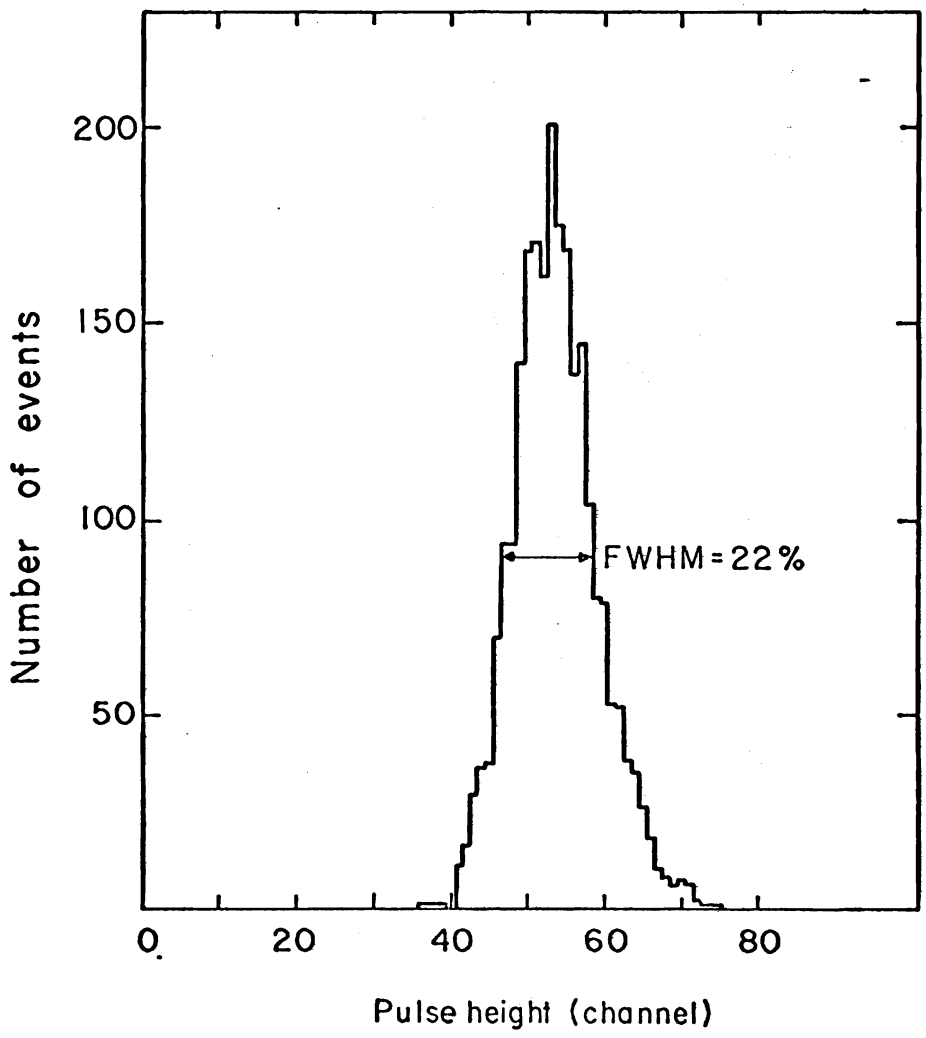
200
150
100
50
0
20
40
60
80
Number of events
Pulse height (channel)
FWHM = 22%

Fig. 5

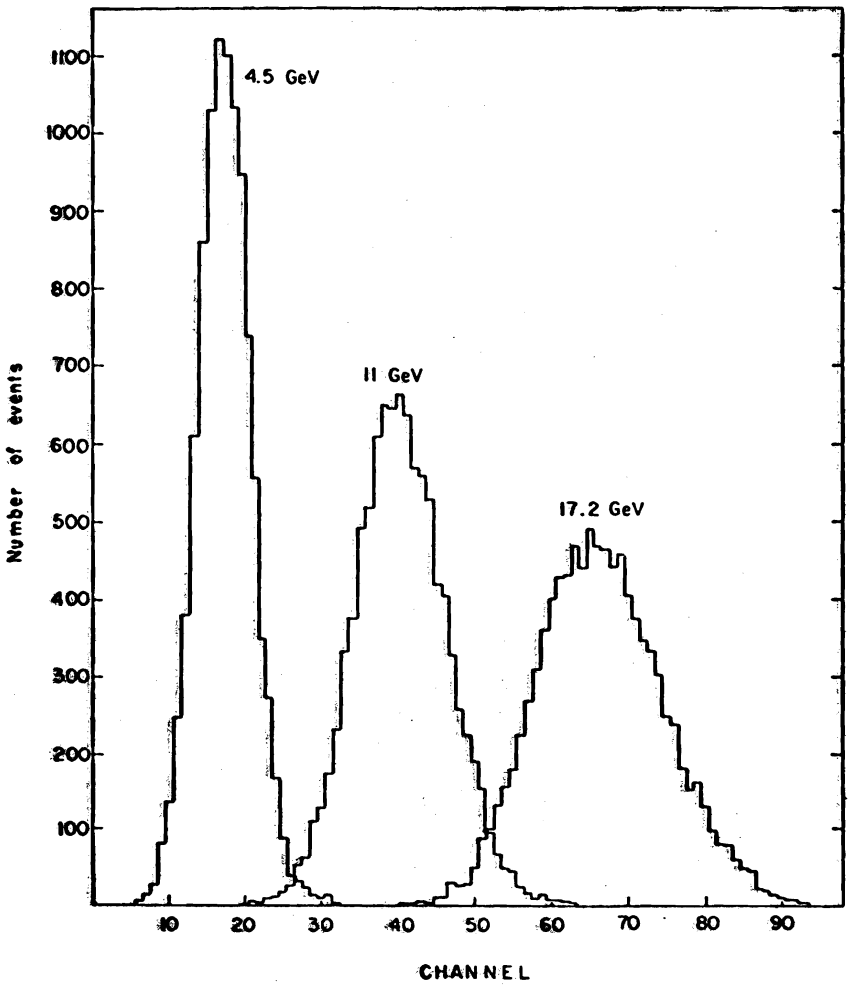
4.5 GeV
11 GeV
17.2 GeV
Number of events
CHANNEL
1100
1000
900
800
700
600
500
400
300
200
100
10
20
30
40
50
60
70
80
90

Fig. 6

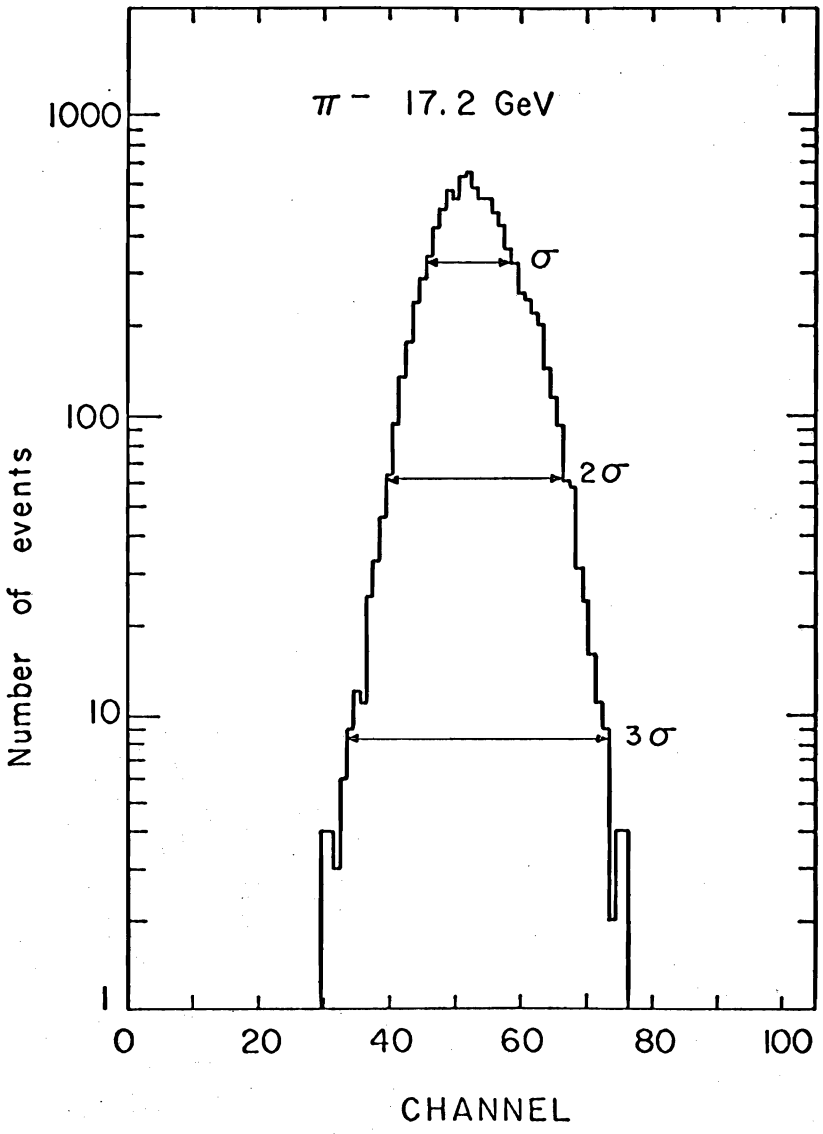
π⁻ 17.2 GeV
σ
2σ
3σ
1000
100
10
1
Number of events
0
20
40
60
80
100
CHANNEL

Fig. 7

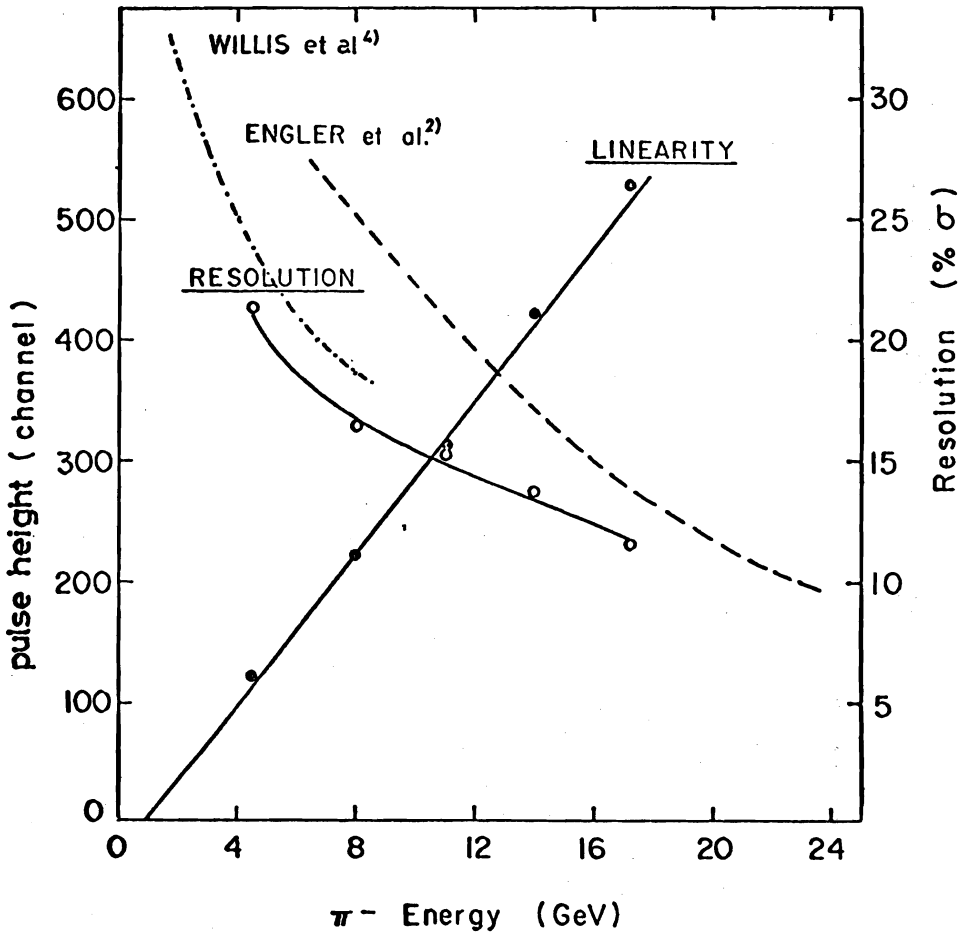
WILLIS et al 4)
ENGLER et al.2)
LINEARITY
RESOLUTION
pulse height (channel)
Resolution (% σ)
π⁻ Energy (GeV)
0
100
200
300
400
500
600
5
10
15
20
25
30
0
4
8
12
16
20
24

Fig. 8

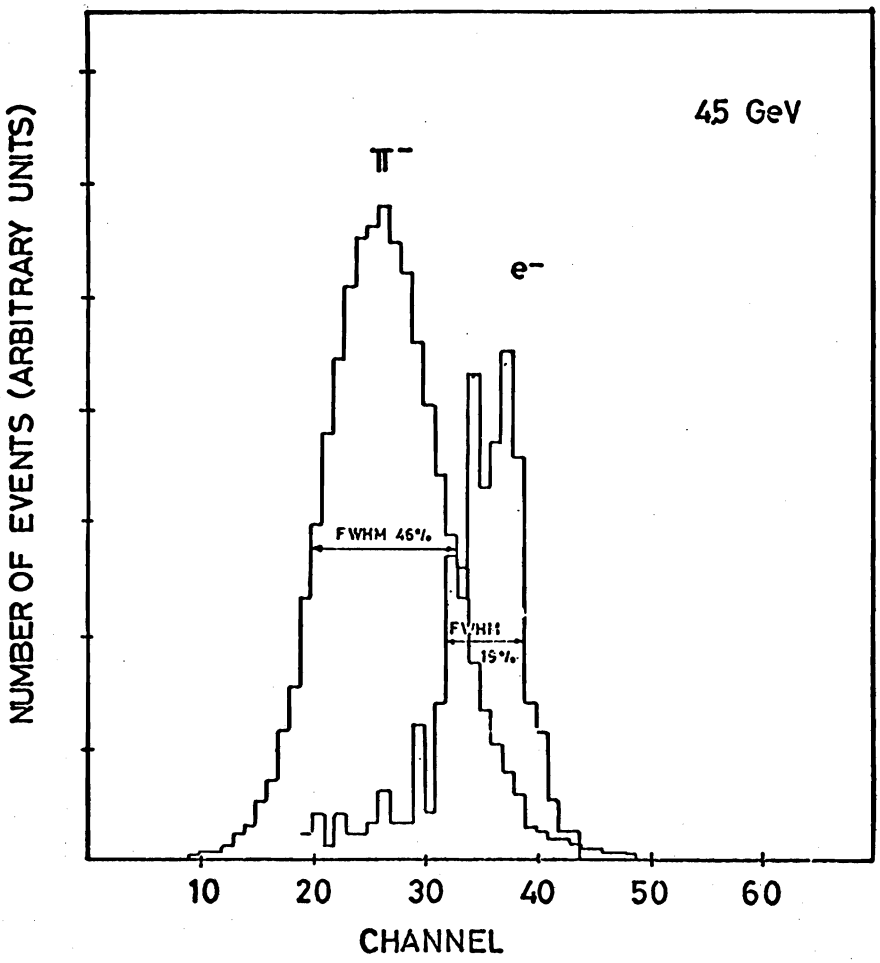
45 GeV
π⁻
e⁻
FWHM 46%
FWHM
15%
NUMBER OF EVENTS (ARBITRARY UNITS)
10
20
30
40
50
60
CHANNEL

Fig. 9

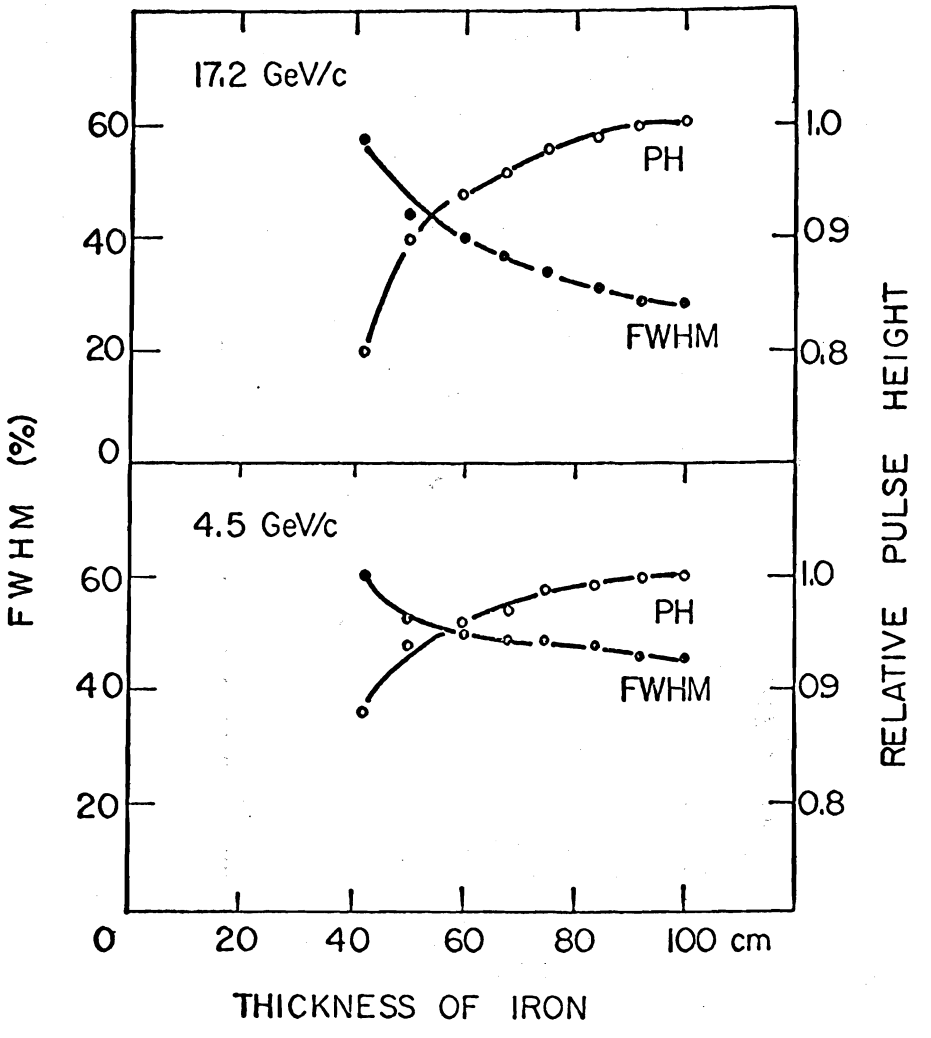
17.2 GeV/c
PH
FWHM
4.5 GeV/c
PH
FWHM
60
40
20
0
1.0
0.9
0.8
20
40
60
80
100 cm
FWHM (%)
RELATIVE PULSE HEIGHT
THICKNESS OF IRON

Fig. 10

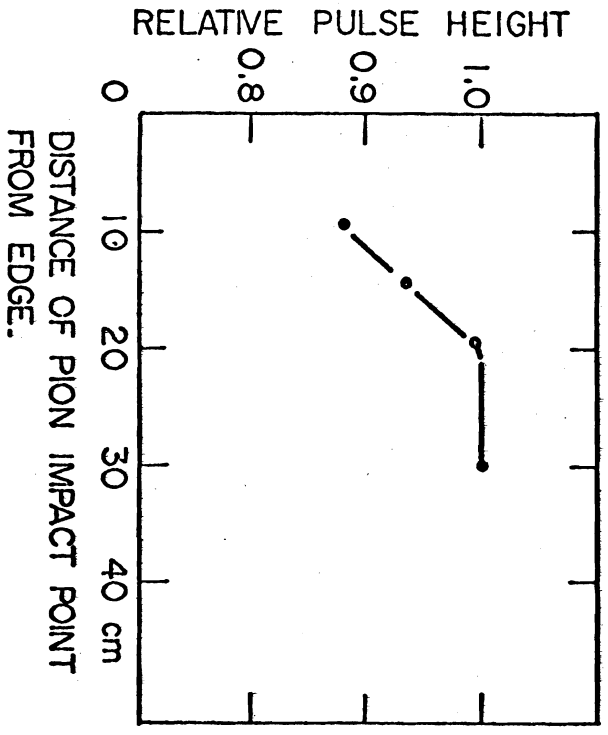
RELATIVE PULSE HEIGHT
0.8
0.9
1.0
0
10
20
30
40 cm
DISTANCE OF PION IMPACT POINT
FROM EDGE.

Fig. 11

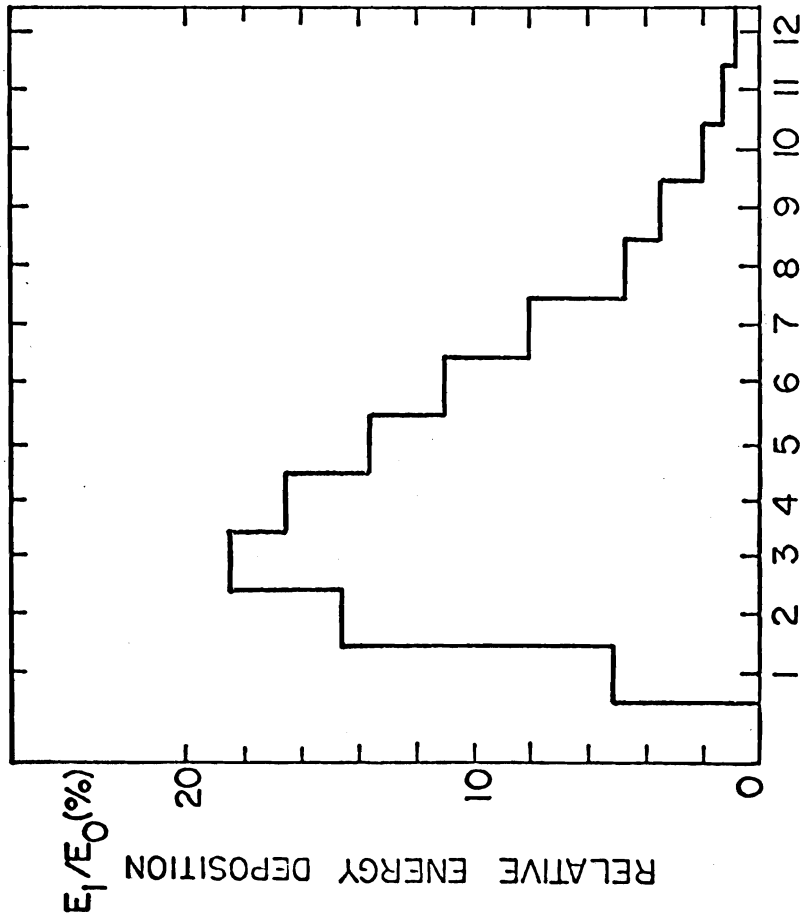
RELATIVE ENERGY DEPOSITION
E_1/E_0(%)
0
10
20
1 2 3 4 5 6 7 8 9 10 11 12
MODULE

Fig. 12

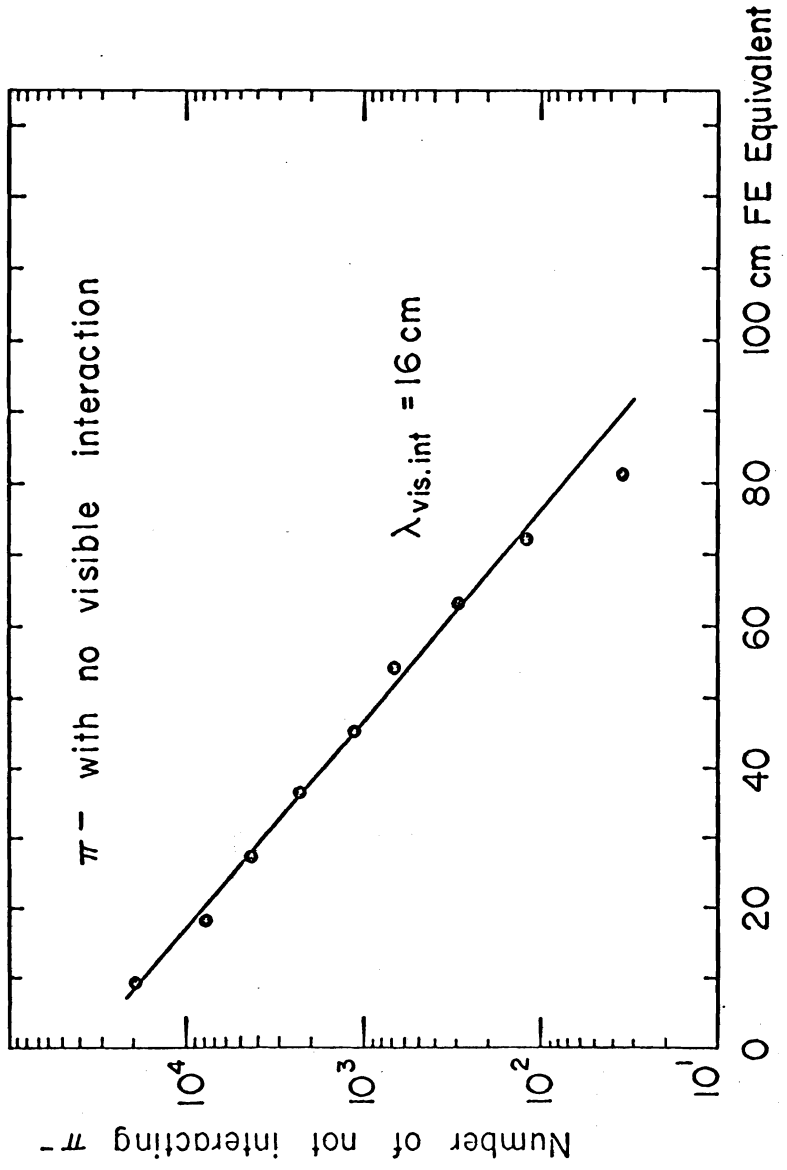
Number of not interacting π⁻
10⁴
10³
10²
10¹
0
20
40
60
80
100 cm FE Equivalent
Traversed thickness
π⁻ with no visible interaction
λvis.int = 16 cm

Fig 13

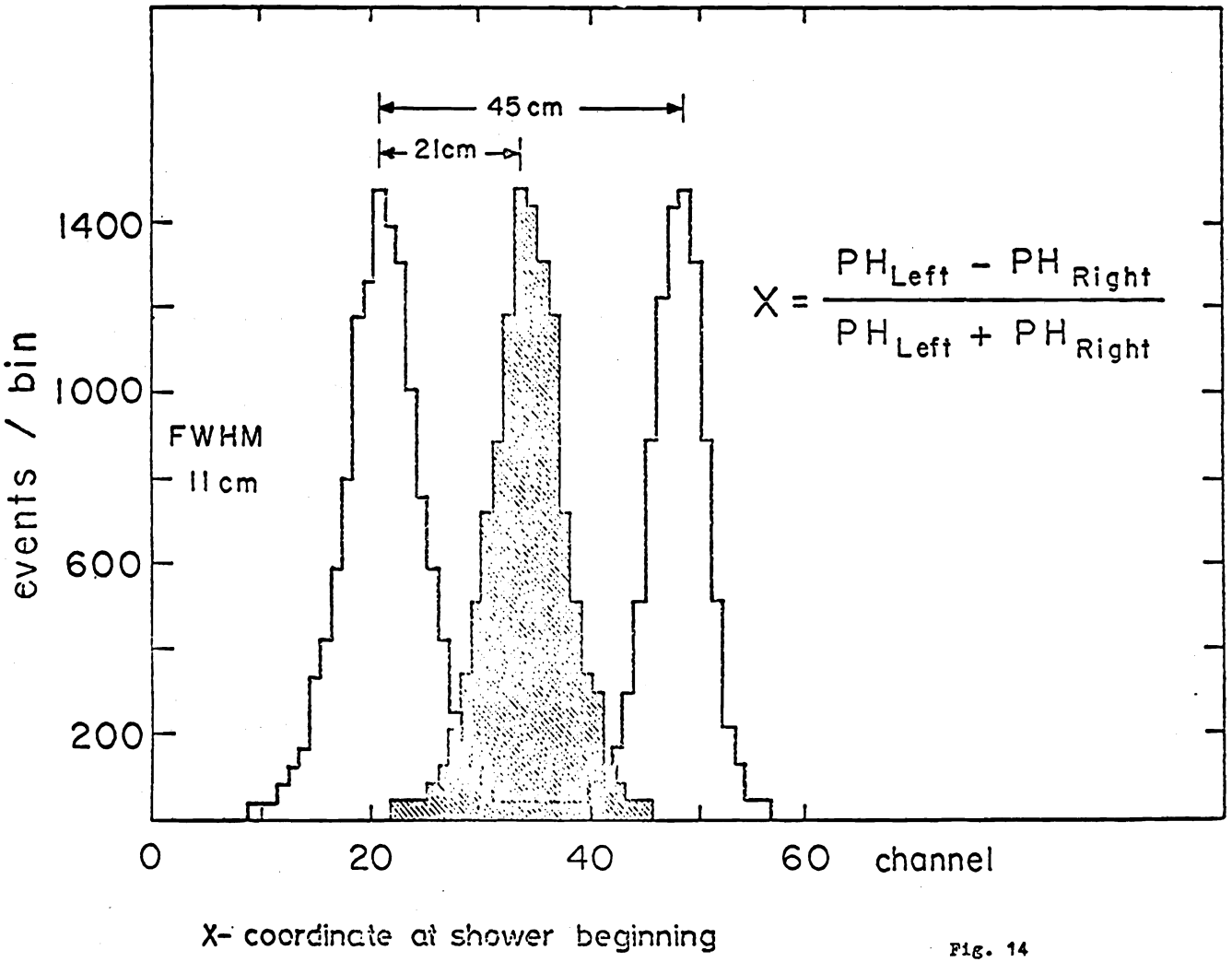
45 cm
21cm
1400
1000
600
200
events / bin
FWHM
11 cm
$X = \frac{PH_{Left} - PH_{Right}}{PH_{Left} + PH_{Right}}$
0
20
40
60
channel
X- coordinate at shower beginning

Fig. 14